Conf-941203--16

SAND94-1557C

A STATISTICAL ANALYSIS OF THE EFFECT OF PECVD DEPOSITION PARAMETERS ON SURFACE AND BULK RECOMBINATION IN SILICON SOLAR CELLS

D. S. Ruby
Sandia National Laboratories
Albuquerque, NM 87185-0752

W. L. Wilbanks and C. B. Fleddermann
University of New Mexico
Albuquerque, NM 87131-1356

ABSTRACT

We have performed a statistically designed multiparameter experiment using response surface methodology to determine the optimum deposition and anneal conditions for PECVD silicon-oxide and silicon-nitride films on Si solar cells. Our process includes a unique *in situ* hydrogen plasma treatment to promote bulk defect passivation independently of surface effects. Our goal has been to define a process to optimize cell performance by minimizing recombination while also providing an effective antireflection coating. Our initial results show that excellent emitter-surface passivation, approaching that of the best thermally grown oxides, can be obtained using a single-layer nitride coating whose refractive index is optimized for antireflection purposes. Use of the PECVD-nitride instead of a TiO_2 ARC resulted in an 11% increase in output power.

INTRODUCTION

The use of Plasma-Enhanced Chemical Vapor Deposition (PECVD) as a low-temperature surface passivation technique for silicon solar cells is a topic of increasing importance. PECVD is now widely recognized as a potentially cost-effective, performance-enhancing technique that can provide surface passivation and produce an effective antireflection coating layer at the same time [1]. For some solar-grade silicon materials, it has been observed that the PECVD process results in the improvement of bulk minority-carrier diffusion lengths as well, presumably due to bulk defect passivation [2].

While previous results show that certain deposition and annealing conditions can be effective, no one has yet reported a systematic optimization of deposition and annealing parameters for solar-grade silicon materials. We have therefore performed a statistically designed experiment using response surface methodology to predict the optimum deposition and anneal conditions, and then tested the prediction by fabricating solar cells on cast multicrystalline solar-grade silicon.

EXPERIMENTAL PROCEDURE

We began our investigation with a main-effects experimental design to determine which parameters had the most effect on emitter-surface recombination. In this way, we intended to reduce the large number of factors by identifying those with the most influence on cell performance. Then, a quadratic interaction experiment was done to find optimum combinations of parameters which minimize emitter recombination and optimize refractive index.

The depositions were performed using a modified Pacific Western Coyote PECVD reactor. This is a commercial, RF parallel-plate reactor operating at 13.56 MHz with large batch-size and high-throughput potential. Reaction gases for nitride deposition were a 3% mixture of silane in nitrogen, pure ammonia, and nitrogen diluent, while nitrous-oxide was used instead of ammonia for oxide depositions.

We initially carried out the depositions on high-lifetime float-zone (FZ) single-crystal wafers that had the same lightly diffused phosphorus emitters we use in our high-efficiency solar cells. We chose this as an experimental vehicle because we can measure emitter saturation-current density (J_{oe}) on these structures and calculate the front-surface recombination velocity without having to fabricate a large number of complete solar cells [3,4].

RESULTS

Main-Effects Experiments

The parameters investigated in the nitride main-effects experiment are shown in Table 1. Because atomic hydrogen generated in the PECVD deposition of silicon oxides and nitrides is thought to play a critical role in the ability of these layers to provide surface and bulk passivation, we included the introduction of a hydrogen-plasma wafer cleaning step before the film deposition as one of the parameters to be investigated. We also included the introduction of hydrogen gas during the film deposition, so we could have independent control over the amount of hydrogen present in the plasma. The other

---

This work was supported by the U. S. Department of Energy under contract DE-AC04-94AL85000.

DISTRIBUTION OF THIS DOCUMENT IS UNLIMITED

ac

variables, including post-deposition forming gas anneal (FGA) temperature are listed in the table.

Table 1. Parameters used for the Silicon-Nitride and Silicon-Oxide Main-Effects Experiments

Parameter [units]	Min Value	Max Value
Hydrogen plasma pre-clean time [min]	0	10
Substrate temp. during deposition [°C]	250	300
Silane/ammonia flow ratio [sccm/sccm]	10	16
Ammonia flow rate [sccm]	19	56
Silane/N_2O flow ratio [sccm/sccm]	0.87	1.62
Nitrous Oxide flow rate [sccm]	138	553
Diluent nitrogen flow rate [sccm]	0	300
H_2 flow rate during deposition [sccm]	0	404
RF-power applied to plasma (nitride) [W]	47	83
RF-power applied to plasma (oxide) [W]	47	70
Temp. of post-deposition FGA [°C]	350	400

The results of the main-effects experiments in Figs. 1 and 2 show that the emitter surface passivation provided by either PECVD oxides or nitrides can range from almost as poor as a bare or TiO_2-covered silicon surface to almost as good as the best thermal-oxide-passivated surface. Unpassivated TiO_2-covered cells are typical of those from the commercial Si-PV industry.

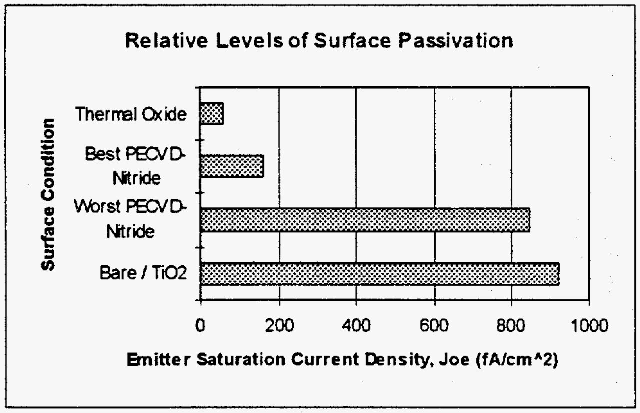

Figure 1. Range of J_{oe} values obtained in the nitride main-effects experiment, measured at 25°C.

The results of the main-effects experiments showed that the FGA temperature had the largest effect on J_{oe} for both oxides and nitrides, with the lower temperature being strongly preferred. The higher deposition temperatures produced better passivation for both film types. Interestingly, the hydrogen-plasma pre-clean resulted in higher J_{oe} values for both films, possibly because of damage to the surfaces of the float-zone wafers used. This effect may be outweighed by beneficial passivation of bulk defects when this factor is studied on mc-Si cells.

The other factors had smaller, but significant effects, such as the RF-power, where lower power was preferred for the nitrides, but higher power for the oxides. In the case of the nitrides, the gas ratios and rates were significant, but for the oxides, they were not. This may be because the oxide always tends to be deposited as SiO_2 with a fixed refractive index of 1.5, while the stoichiometric ratio and refractive index for the nitride is a function of the gas rates. The addition of hydrogen during the deposition resulted in slightly higher J_{oe} values for the nitrides, but slightly lower values for the oxides.

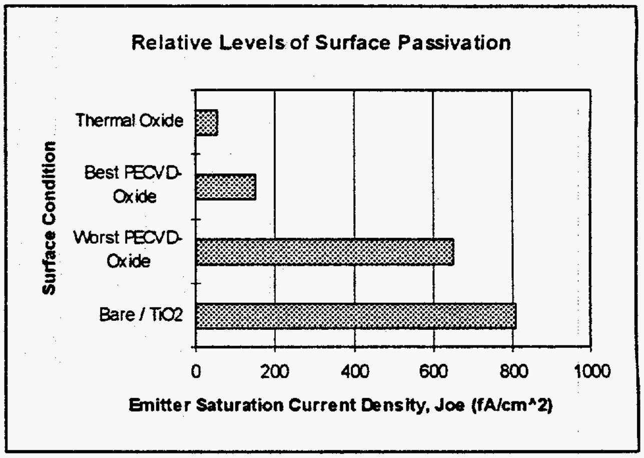

Figure 2. Range of J_{oe} values obtained in the oxide main-effects experiment, measured at 25°C.

We used this information to plan the quadratic experiments that followed. In order to keep the number of trials to a manageable level, we restricted the factors used to the four that had the largest effect on J_{oe}, and eliminated the detrimental hydrogen pre-cleans.

Quadratic Experiments

We first performed the oxide quadratic experiment using parameters similar to those in Table 1, except with the lower limit of the FGA temperature set to 300°C, since the lower temperature was so strongly preferred earlier. The SiH_4 / N_2O ratio was set to 0.5 and the N_2O rate was set to 400 sccm. We used a statistical analysis program to calculate the functional dependence of J_{oe} on the four factors varied, assuming a dependence of the form:

$$J_{oe} = b_0 + \Sigma\, b_i x_i + \Sigma\, b_{ij} x_i x_j + \Sigma\, b_{ii} x_i^2 \quad \text{,for } i = 1 \text{ to } 4,\ j > i \qquad (1)$$

The result of this calculation is shown in a contour plot of the response surface in Fig. 3. Figure 4 shows the lowest and highest measured values of J_{oe} from the best and worst trials, respectively, the measured thermally oxidized and bare wafer extreme values, and compares these with the program's predicted optimized value. The optimized PECVD-oxide is still not as good as the thermal oxide.

Because the lowest FGA temperature was so strongly preferred, we chose to fix the FGA temperature at 300°C for the nitride quadratic experiment. The diluent nitrogen and hydrogen flow rates were both set to zero. The

contour plots for both J_{oe} and refractive index of the nitride films are shown in Figures 5 and 6.

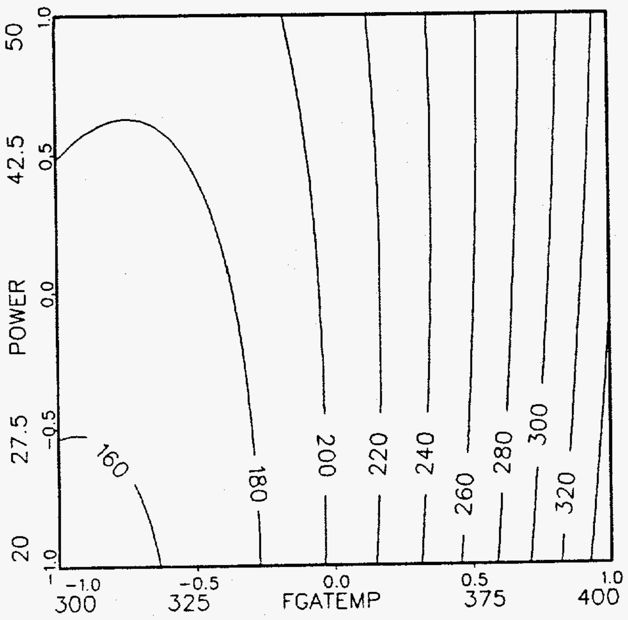

Figure 3. Contours of constant J_{oe} [fA/cm^2] for PECVD-oxide films on the response surface, which predicts a minimum value in the lower left corner.

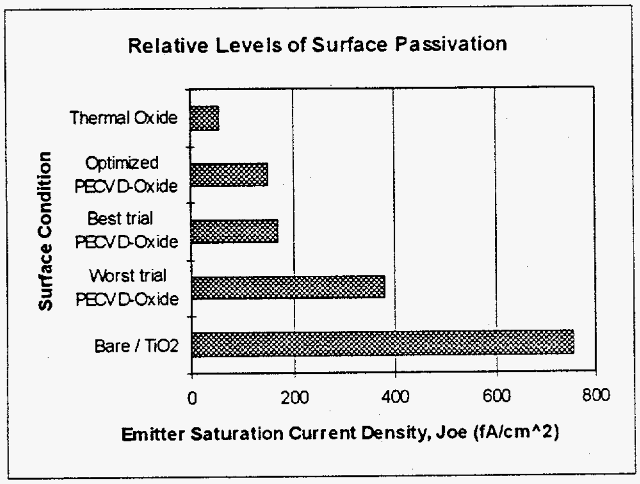

Figure 4. The measured and predicted J_{oe} values for the oxide quadratic experiment.

The analysis predicted that deposition conditions existed where both the emitter recombination could be minimized and the refractive index could be maximized at a value of 2.3, which is optimum for a single-layer AR coating on a Si cell encapsulated under glass.

Figure 7 shows the measured values of J_{oe} from the best and worst trials, the measured thermally oxidized and bare wafer values, and the predicted optimized value.

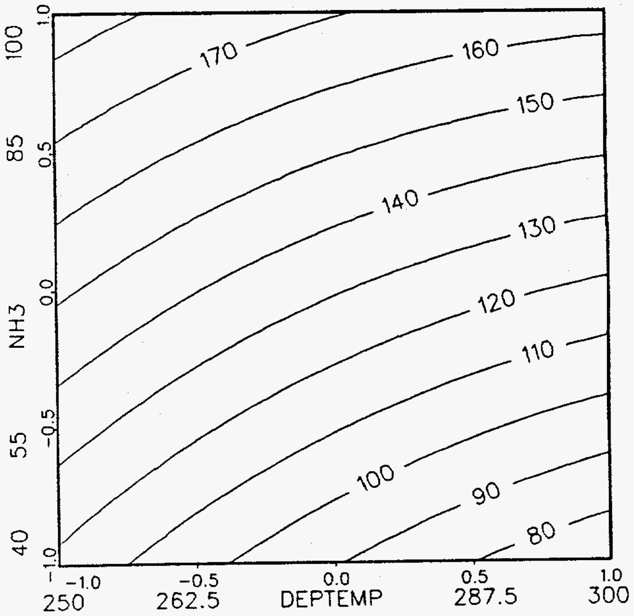

Figure 5. Contours of constant J_{oe} [fA/cm^2] for PECVD-nitride films on the response surface, which predicts a minimum in the lower right corner.

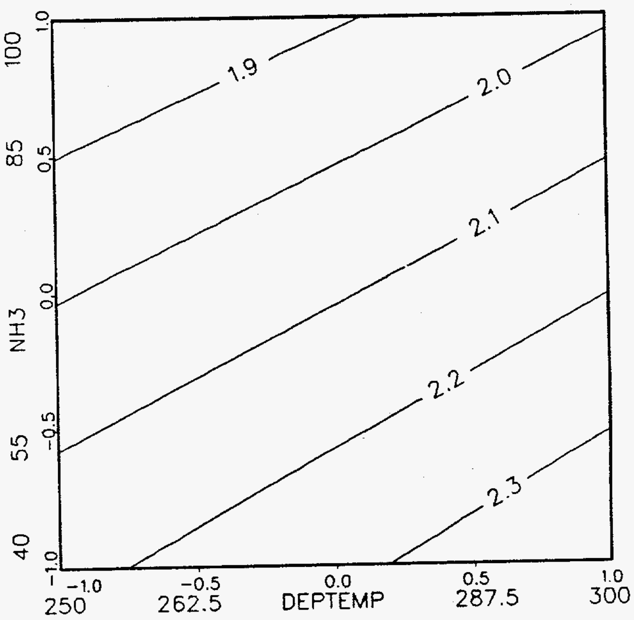

Figure 6. Contours of constant refractive index for PECVD-nitride films on the response surface, which predicts a maximum in the lower right corner.

Solar Cell Fabrication

The analysis predicted that the optimized nitride conditions should produce a film with surface passivation properties almost as good as that of our best thermal oxides, while at the same time producing optimal ARC properties. We tested this prediction by fabricating solar cells on float-zone wafers and also on cast mc-Si wafers provided by Solarex Corp. Figure 8 shows measured internal quantum efficiency curves for the same surface conditions of Figure 7, where the optimized curve here represents measured IQE data on a cell fabricated using the predicted best deposition conditions.

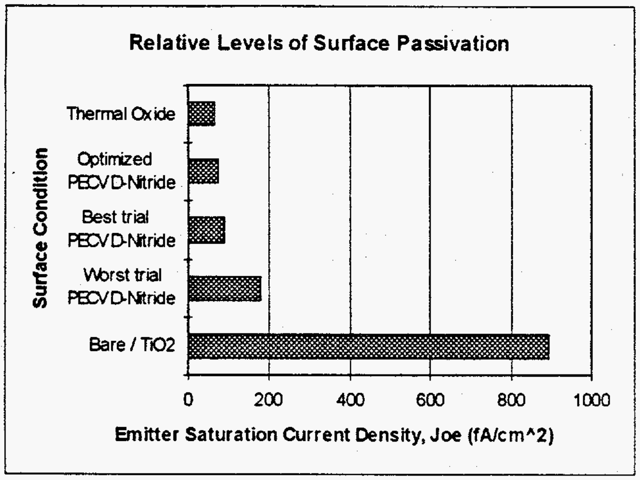

Figure 7. The measured and predicted J_{oe} values for the nitride quadratic experiment.

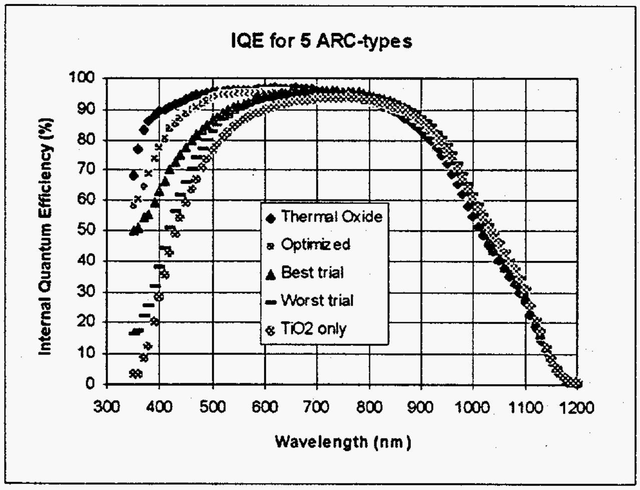

Figure 8. Measured IQE curves on mc-Si cells for the same five surface conditions shown in Fig. 7.

Figure 8 shows a continuous improvement in the blue response of nitride-passivated cells as the deposition conditions approach those of the optimized case. This is entirely consistent with the lower J_{oe} values measured earlier and proves that the conditions predicted to be optimized do indeed result in better-passivated emitters, even on mc-Si cells. Also, there is no degradation in red response from the plasma, and future work will determine if the addition of hydrogen results in long-wavelength improvement.

Finally, Figure 9 shows the measured short-circuit current densities of the mc-Si and float-zone Si cells fabricated using the same surface conditions as in Fig. 7.

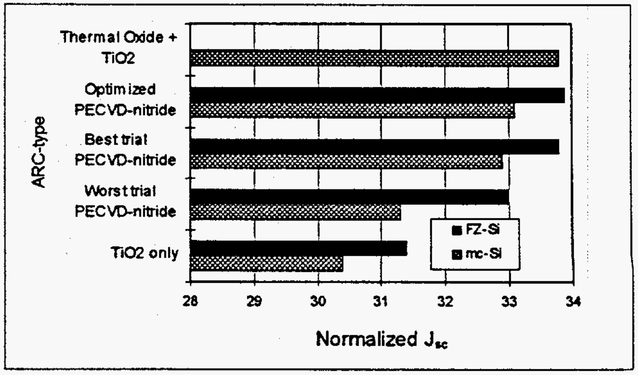

Figure 9. Measured short-circuit current densities, normalized to the same reflectance, for the surface conditions of Figs. 7 and 8, for mc-Si and FZ-Si cells.

CONCLUSIONS

The choice of deposition and anneal conditions had a large impact on the quality of PECVD emitter passivations. A set of conditions was found which provides excellent surface passivation and optimum ARC properties from a single-layer nitride film, resulting in a 9% increase in current and 2% increase in open-circuit voltage compared to a TiO_2 layer.

ACKNOWLEDGEMENTS

The authors would like to thank K. Wroblewski for much of the PECVD equipment characterization that was done, and for performing the main-effects depositions. Many thanks go to B.L. Silva, M.E. Buck and J.W. Tingley for the cell and wafer processing. We are also grateful to L. Irwin and J.K. Snyder for the many cell measurements.

REFERENCES

[1] Z. Chen, P. Sana, J. Salami, and A. Rohatgi, "A Novel and Effective PECVD SiO_2/SiN Antireflection Coating for Si Solar Cells," *IEEE Trans. Elect. Dev.*, **40**, June 1993, pp. 1161-1165.

[2] J. Szlufcik *et al.*, "Improvement in mc-Si Solar Cells after Thermal Treatment of PECVD Silicon Nitride AR Coating," *Proc. 12th European PV Solar Energy Conf.*, 1994, pp. 1018-1021.

[3] D. S. Ruby and J. D. Levine, "Low-Temperature Emitter-Passivation for Silicon Solar Cells," *Proc. 11th European PV Solar Energy Conf.*, 1992, pp. 385-388.

[4] P.A. Basore and B.R. Hansen, "Microwave-Detected Photoconductance Decay," *21st IEEE PVSC,* 1990, pp. 374-379.